Semnan University

Journal of Modeling & Simulation in Electrical & Electronics Engineering (MSEEE)

Journal homepage: **https://mseee.semnan.ac.ir/**

ISSN: 2821-0786

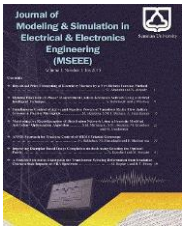

Co-Optimization of Conservation Voltage Reduction and Uncertainty-Aware Demand Response: A Hybrid IGDT-Fuzzy Programming Approach

Hamid Helmi[1], Leila Mohammadian[1]* and Taher Abedinzadeh[1]*

***Abstract*-- The integration of distributed generation and demand response programs introduces significant complexity to microgrid management. This paper proposes a comprehensive, stochastic framework for the day-ahead scheduling of a microgrid that simultaneously co-optimizes Demand Response Programs (DRPs) and a Conservation Voltage Reduction (CVR) strategy. The model aims to enhance operational performance, improve reliability, and minimize costs. To address the inherent uncertainties of renewable generation, the framework employs both Time-of-Use (TOU) and incentive-based DRPs, creating a vital link between variable generation and flexible demand. This is complemented by CVR implementation, which leverages voltage-dependent load modeling to achieve further peak load reduction. A key feature of the approach is the use of Information Gap Decision Theory (IGDT) to rigorously model generation uncertainty, providing a robust decision-making foundation. The optimization problem is solved using a Genetic Algorithm (GA) on a test system. Simulation results confirm that the coordinated application of uncertainty-aware DRPs and CVR leads to a substantial reduction in operational costs while significantly improving key microgrid reliability indices, demonstrating the efficacy of the proposed integrated framework.**

***Index Terms*- Active Distribution Networks, Conservation Voltage Reduction(CVR), Demand Response Program(DRP), Information Gap Decision Theory(IGDT), Multi-Objective Optimization.**

I. INTRODUCTION

The global energy landscape is undergoing a profound transformation, driven by the dual imperatives of decarbonization and grid modernization. This transition is characterized by the massive integration of Distributed Energy Resources (DERs), particularly renewable energy sources, such as solar PV and wind power, alongside the rapid electrification of transportation through Electric Vehicles (EVs) [1]-[2]. Microgrids have emerged as a pivotal technology to manage these diverse resources, offering localized control, enhanced resilience, and improved operational efficiency [3]-[4]. However, the inherent intermittency of renewables and the significant, spatially-temporal variable load introduced by EV charging pose substantial challenges to the stable, secure, and economic operation of both microgrids and the main distribution grid [5]-[6].

To address these challenges, sophisticated day-ahead operation planning is paramount. This process forms the backbone of microgrid energy management, aiming to determine the optimal set-points for all controllable assets [7]. Two key strategies have proven highly effective in enhancing operational flexibility and efficiency: Demand Response (DR) and Conservation Voltage Reduction (CVR). DR programs incentivize end-users to adjust their consumption patterns, providing the necessary flexibility to balance generation and load, thereby mitigating the effects of uncertainty in renewable generation and load forecasts [8]-[9]. CVR, a well-established voltage regulation technique, leverages the voltage-dependent nature of certain loads to reduce both energy consumption and peak demand by strategically operating the distribution system at the lower end of the permissible voltage band [10]-[11]. The synergy between DR and CVR can unlock significant potential for energy savings, peak shaving, loss reduction, and improved voltage stability [12]-[13].

Received; 2026-03-04 Revised; 2026-06-14 Accepted; 2026-08-23
1. Department of Electrical Engineering, Shab.C., Islamic Azad University, Shabestar, Iran.
*Corresponding author Email: le.mohammadian@iau.ac.ir, Taher.abedinzadeh@iau.ac.ir

Cite this article as:
Mohammadian, L., Abedinzadeh, T., and Helmi, H. (2026) Co-Optimization of Conservation Voltage Reduction and Uncertainty-Aware Demand Response: A Hybrid IGDT-Fuzzy Programming Approach. *Journal of Modeling & Simulation in Electrical & Electronics Engineering (MSEEE). Semnan University Press . 6 (4), 69-85.*
DOI: https://doi.org/10.22075/mseee.2026.40785.1259

© 2026 The Author(s). Journal of Modeling & Simulation in Electrical & Electronics Engineering is published by Semnan University Press. This is an open-access article under the CC-BY 4.0 license. (https://creativecommons.org/licenses/by/4.0/)

Despite individual advancements, integrating CVR effects with uncertainty-based DR into a unified, multi-objective day-ahead optimization framework for modern active distribution networks and microgrids remains a complex challenge. This is particularly true for systems with high penetrations of EVs [14]-[15], which introduce new dimensions of uncertainty and load flexibility. Furthermore, the co-optimization of traditional assets with advanced power electronics interfaces, such as Smart Transformers and Soft Open Points (SOPs), alongside CVR and DR, is essential for unlocking the full potential of active network management [16] - [17]. This paper proposes a comprehensive, two-stage fuzzy-based optimization framework to address this multifaceted problem, aiming to simultaneously achieve economic and technical objectives for a resilient and efficient distribution system.

DR is a cornerstone of modern smart grid operation, essential for balancing supply and demand under uncertainty. A comprehensive survey of DR programs, outlining various pricing methods and optimization algorithms, was provided in [8]. The application of DR in microgrids has been extensively studied. A day-ahead optimal bidding strategy for a microgrid, incorporating a DR program to manage uncertainties and outages of renewable resources, was developed in [9]. The challenge of uncertainty in multi-microgrid systems has been addressed through various approaches. A data-driven peer-to-peer (P2P) energy exchange model for grid-interconnected multi-microgrids was proposed in [18]. Similarly, optimal power scheduling and energy management in systems with high renewable penetration were focused on in [19]-[20], emphasizing energy trading and storage optimization. An adaptive and predictive energy management strategy for real-time optimal power dispatch from Virtual Power Plants (VPPs) was presented in [21], highlighting the need for sophisticated control in systems integrated with renewables and storage. Recent studies continue to advance this field. For instance, a distributionally robust optimization framework for DR was introduced in [22], effectively handling ambiguous probability distributions of renewable generation. Similarly, a novel deep reinforcement learning approach for real-time DR management in microgrids with high PV penetration was developed in [23], demonstrating superior performance in uncertain environments.

The integration of EVs into the power grid is a critical area of research. Early works recognized their potential impact, and recent studies focus on their management as a flexible resource. A techno-economic solution for demand control in ports using Energy Storage Systems (ESS), a context relevant to high-power EV charging, was presented in [24]. A coordinated EV management system, specifically for providing grid-support services in residential networks, treating EVs as an active grid asset, was previously designed. Research on EV charging infrastructure has also advanced. Optimization schemes for grid-tied PV-battery charging stations, focusing on power allocation, charging coordination, and grid support, were proposed in [25]-[26]. The aggregation of EV flexibility is crucial; an equivalent time-variant storage model to harness the flexibility of an EV fleet through forecasting and aggregation was developed in [27]. Furthermore, the energy management of EV parking lots under peak load reduction-based DR programs was optimized in the literature, explicitly considering uncertainty. Energy management systems for residential buildings with EVs and DERs, as well as rule-based strategies for hybrid energy storage in plug-in hybrid EVs, were explored in [28] and [29], respectively. The latest research explores the aggregation of vehicle-to-grid (V2G) services from fleets of autonomous EVs, proposing a bi-level market framework that significantly enhances grid flexibility [30].

Energy storage is a key enabler for mitigating intermittency and enhancing flexibility. A real-case analysis of a BESS used for energy time shift, demand management, and reactive power control, demonstrating practical applications, was presented in [31]. A market-based energy management model for a building microgrid that considers battery degradation, adding a crucial techno-economic dimension, was proposed in [32]. Advanced control strategies are vital for managing these complex systems. Model Predictive Control (MPC) was utilized for real-time energy management in hybrid energy storage systems and energy hubs integrated with EVs and RES in [33]-[34], respectively, highlighting the trend towards predictive, closed-loop optimization. A design framework for privacy-aware demand-side management with a realistic energy storage model was introduced in [35]. A recent study presents a federated learning-based MPC for multi-microgrid systems, addressing data privacy concerns while maintaining operational efficiency, representing a significant step forward in secure, distributed control [36].

CVR is a well-known technique for energy conservation and peak demand reduction. Its integration with modern grid applications is a growing research area. The impacts of co-optimizing CVR and DR operations within a bi-level market-clearing model with dynamic nodal pricing were investigated in the literature, demonstrating significant interactions between the two. A risk-averse Volt-VAr management scheme that coordinates DERs with a DR program, an approach that inherently involves voltage regulation principles akin to CVR, was proposed in [13]. The concept of coordinated optimization is expanding to include a wider set of assets and objectives. An integrated DR framework for microgrids with an incentive-compatible bidding mechanism was proposed in [37]. The optimal energy management of grid-connected multi-microgrid systems considering demand-side flexibility via a two-stage multi-objective approach was studied in [38]. Optimal microgrid programming based on ESS, price-based DR, and distributed renewables was focused on in [39]. A very recent paper proposes a joint optimization of CVR and SOPs in unbalanced distribution networks, using a multi-agent deep reinforcement learning approach to dynamically manage voltages and power flows, showcasing the next frontier in integrated voltage control [40].

A thorough analysis of the literature reveals a clear progression towards more integrated and sophisticated energy management systems. However, a critical gap persists in developing a holistic day-ahead operation planning model that seamlessly unifies CVR optimization with uncertainty-based DR programs for flexible loads and EVs, while also coordinating advanced assets such as SOPs and smart transformers within a multi-objective framework. Many studies consider DR and EVs, but omit the explicit modeling and co-optimization of CVR as a continuous control variable. Others address CVR or asset coordination without fully leveraging the comprehensive flexibility of uncertainty-based DR programs

tailored for modern loads such as EVs in a multi-objective setting. Furthermore, a unified approach that jointly minimizes operational cost, improves voltage stability, minimizes voltage deviation, and reduces feeder loading through the coordinated action of CVR, DR, SOPs, and smart transformers has not yet been fully explored.

Building upon the foundational work in the field, this paper introduces a novel two-stage fuzzy multi-objective optimization framework for the day-ahead operation of an active distribution network. The key contributions of this work are:

1. The development of an integrated model that explicitly co-optimizes CVR operation, uncertainty-based DR for flexible loads and EVs, and the set-points of a Smart Transformer and an SOP.
2. The application of a fuzzy-based goal programming approach to find a Pareto-optimal compromise solution between conflicting economic (operational cost) and technical (Voltage Stability Index, Average Voltage Deviation, feeder loading) objectives.
3. A comprehensive validation on a modified IEEE 69-bus test system, demonstrating the effectiveness of the proposed strategy in achieving a superior balance between competing operational goals compared to single-objective scenarios.

The remainder of this paper is organized as follows. In Section 2, Problem modeling and notations, including the objective functions and constraints, as well as the proposed approach for CVR and optimization algorithm, are described. The results of the simulation and analysis are presented in Section 3. Finally, Sections 4 and 5 discuss and conclude the paper, respectively.

II. Modeling the Problem and Notations

A. Notations

TABLE I
Indices, Functions, Variables, and Parameters

	Indices
i	Generators
t	Time
nWT	The number of wind turbines
	Functions
f_i^{WT}	The conversion function of wind speed to wind turbine generation
f_i^{PV}	The conversion function of the radiation value into photovoltaic generation
	Variables
revenue	Revenue
Reliability	Reliability
$income$	Income
$cost$	Cost
$P_{i,t}$	The generation rate of unit i at time t
$Cost_{gen}$	Generation cost
$Cost_{res}$	Spinning reserve cost
$Cost_{rel}$	Reliability cost
$U_{i,t}$	Binary variable of starting unit i at time t
$K_{i,t}$	Binary variable of unit i being turned on at time t
$\Delta P_{s,t}$	Change in available power due to events at time t
$\Delta R_{s,t}$	Change of available reservation due to events at time t
R_t	Total reservation at time t
$p_{s,t}$	The probability of event "s" at time t
$b_{s,t}$	Binary variable of load shedding due to event "s" at time t
$C(t)$	The energy in the battery at time t
$EENS$	The expected amount of energy not supplied
$LOLP$	The possibility of load-shedding
$R_{i,t}$	The amount of reservation of unit i at time t
P_t^E	Battery generation or consumption power
	Parameters
$C_{i,t}$	Baseline generation cost per MW
$q_{i,t}$	Spinning reservation cost per MW
SC_i	The cost of setting up unit "i"
$VOLL$	Lost load value
$LOLP_t^{max}$	The maximum probability of acceptable load shedding at time t
P_t^D	Load value at time t
P_i^{max}	Generation capacity of unit i
P_i^{min}	The minimum generation by unit i
RUR_i	The maximum slope of the increase in the generation by unit i
τ	Time steps

$v_{i,t}^{actual}$	The actual wind speed value at time t
$v_{i,t}^{fcst}$	The forecasted wind speed value at time t
$g_{i,t}^{fcst}$	The forecasted radiation value at time t
$g_{i,t}^{trun}$	The actual radiation value at time t
P_{max}^{E}	The maximum battery capacity
d_T	Battery charge efficiency
C_S	Initial battery charge
C_E	Final battery charge
C_{min}	The minimum battery capacity
C_{max}	The maximum battery capacity
du_T	Duration of each failure

B. The baseline model of the objective function and constraints

An optimization problem with an objective function and specific constraints is developed in this study. Due to the problem's relevance to short-term studies of the power system, its solution time is a crucial factor. Numerical results show that the solution time of a problem is proportional to the time horizon, according to the proposed algorithms. The multi-objective framework of this model can be expressed by (1), which takes revenue and reliability as two objectives

$$\max(\text{revenue}, \text{reliability}). \tag{1}$$

$$\text{revenue} = income - cost \tag{2}$$

$$income = \sum_{t=1}^{T}\sum_{i=1}^{I} MP(t).P_{i,t} \tag{3}$$

$$cost = Cost_{gen} + Cost_{res} + Cost_{rel} \tag{4}$$

$$Cost_{gen} = \sum_{t=1}^{T}\sum_{i=1}^{I}\left[C_{i,t}\left(P_{i,t}, U_{i,t}\right) + SC_i.K_{i,t}\right] \tag{5}$$

$$Cost_{res} = \sum_{t=1}^{T}\sum_{i=1}^{I} q_{i,t}R_{i,t} \tag{6}$$

$$Cost_{rel} = EENS \times VOLL \tag{7}$$

$$\text{Reliability} = LOLP \tag{8}$$

The objective function of the problem consists of two main components, with revenue and reliability as the first and second components, respectively. In this bi-objective problem, the revenue is defined as the difference between income and costs according to (2). The income from selling power to the upstream network forms the income component, as expressed by (3). The total cost includes generation cost, the cost of setting up the units, spinning reserve cost, and reliability cost (4), the first two components of which are expressed by (5) and (6), respectively. Furthermore, the reliability cost, expressed by (7), is equal to load shedding multiplied by the value of the lost load, referred to as the outage penalty or load shedding penalty. The second component of the objective function is reliability. Reliability indices alone cannot express the network's reliability status. On the other hand, the index of expected unsupplied energy can be converted into a cost by multiplying it by the value of the lost load. However, the loss of load probability (LOLP) index is proposed as a separate objective. Accordingly, the developed problem is bi-objective. A maximum value is considered as follows for the load shedding probability index to meet a minimum level of reliability:

$$LOLP_t \leq LOLP_t^{max} \tag{9}$$

where $LOLP_t$ denotes the probability of hourly load shedding, and $LOLP_t^{max}$ is its highest permissible value. This constraint prevents the reliability index from exceeding a specific value.

The proposed framework employs two complementary reliability metrics: LOLP (Loss of Load Probability) as a probabilistic constraint, and EENS × VOLL as a cost-based term in the objective function. The rationale for including both separately is as follows:

- LOLP captures the frequency or probability of load shedding events, which is a regulatory and customer-centric metric. Constraining LOLP ensures that the system does not rely on frequent but small interruptions.
- EENS × VOLL quantifies the expected monetary impact of unsupplied energy, allowing direct trade-off with reserve costs and production costs in the objective function.
  This dual representation enables the operator to simultaneously satisfy a minimum reliability level (via LOLP constraint) while optimizing the economic balance between preventive reserve and outage costs (via EENS × VOLL).

The constraint on the generation and consumption equilibrium is as follows:

$$\sum_{i=1}^{I} P_{i,t} = P_t^D \tag{10}$$

$$\forall t = 1, \ldots, T$$

Since each unit needs to spend a certain amount of time to increase its power, the unit cannot provide the desired amount of reserve:

$$R_{i,t} \leq \min\left(U_{i,t}(RUR_i\tau), P_i^{max}U_{i,t} - P_{i,t}\right) \quad (11)$$

The energy storage system (ESS), or the battery, is a dispatchable unit that simultaneously consumes and generates power. The related technical constraints of this source are as follows:

$$|P_t^E| \leq P_{max}^E \quad (12)$$

$$C(t+1) = C(t) - d_T P_t^{Edc}\eta^E + d_T P_t^{Ec}/\eta^E \quad (13)$$

$$C(0) = C_S\,, C(T) = C_E \quad (14)$$

$$C_{min} \leq C(t) \leq C_{max} \quad (15)$$

where $P_t^{Edc}$and P_t^{Ec} are discharge power and charge power, respectively. P_{max}^E denotes the maximum chargeable or discharge power of the battery and η^E is the charge or discharge efficiency. d_T and $C(t)$ are the duration in hours and the total energy value in the battery until hour t, respectively. C_S and C_E denote the set values of battery energy at the beginning and end of the period, and C_{max} and C_{min} are the maximum and minimum battery capacity. Similar to the battery, the upstream grid can both generate and consume power. The capacity of this grid is limited by the capacity of its transformer communicating with the microgrid. The costs related to supplying power from or selling power to this grid are equal to the wholesale market price.

C. Adding DR to the model

As previously mentioned, two types of DRPs, including incentive-based and TOU programs, are considered in this study. The cost of electricity consumed by subscribers should be reduced after participating in the program compared to the case of not participating. Meanwhile, the comfort level is maintained to check the tendency of the loads to participate in these programs. The DR system's tendency to minimize consumers' electricity costs in each time interval and for the schedule of reduced/shredded loads is shown as follows [6].

$$F_{i/c} = f(x) = min\sum_{t=1}^{T}(PD^t \times x^t \times EP^t) \quad (16)$$

$$0.7 < x^t < 1$$

where EP^t is the price of electricity in each time interval t, PD^t is the electricity demand of shedabble loads at time t. x^t is the decision variable for reducing the load and allowing it to shed a maximum of 30% of the load. In other words, this variable has a value between 0.7 and 1. It is worth mentioning that with each load shedding, an incentive equal to the price of electricity at that moment is given to the corresponding load. The second type of responsive demand is price-based and includes three categories: time of use (TOU), real-time pricing (RTP), and critical peak pricing (CPP). The cost of supplying responsive demands is the TOU program and actual pricing type, and its value is obtained according to (17) and (18) [2].

$$F_{t\&r} = min{:}\,(1-\gamma_1-\gamma_2-\gamma_3)\sum_{t=1}^{T} EP^t * d_0(t) + \sum_{t=1}^{T}\rho(t) * d_e(t) \quad (17)$$

$$d_e(t) = (\gamma_1+\gamma_2+\gamma_3) * d_0(t)(1 + \sum_{k=1}^{T} E(t.k) * \frac{\rho(k) - EP^t}{EP^t}) \quad (18)$$

The percentage of participation in each of these programs is variable; some shiftable loads are contributed in the TOU program, some in the real-time pricing (RTP) program, and some in the CPP program. The sum will be 1. The TOU and CPP programs follow the same equation as (17). The only difference between these two programs is the design of pricing $\rho(k)$ in Eq. (18). In the TOU program, a three-level tariff is considered for off-peak, mid-peak, and on-peak hours, while it changes hourly in the RTP program.

In the above equations, γ_1, γ_2 and γ_3 are the participation rates for the RTP, TOU, and CPP programs in percentage, respectively. de(t) is the consumption of price-sensitive subscribers at hour t after the program, d0(t) is the consumption of shiftable loads before the program, E(t,k) is the price elasticity of hour h compared to hour k, (t)ρ is the electricity tariff at hour t, and 0ρ is the initial price at hour t. The hourly tariff rate and the percentage of subscribers' participation should be determined during the problem for the optimal design of the responsive demand program. The only difference between TOU and RTP programs lies in the type of elasticity matrix, which will be discussed further in the simulation results section.

According to the Cobb-Douglas function, to model the effect of peak pricing on the electricity consumed by subscribers, the consumption of subscribers is considered a function of temperature and price [7].

$$Q(t) = A\,P^{ep}(t)W^{ew}(t) \quad (19)$$

$$A = \gamma_3 * d_0(t) \quad (20)$$

Where *Q*(*t*) is the consumption of loads participating in the critical peak pricing program after the program's implementation, a is the constant coefficient of the load value, which is a percentage of the initial shiftable load, and *P* is the

price of electricity. *W*, *ep*, and *ew* express the ambient temperature, the dependence of charge on price, and the dependence of charge on temperature, respectively. As the price increases, the consumption will decrease and vice versa. Taking the log on both sides of (19) results in (21). The logarithm of each variable is represented in lowercase.

$$q(t) = A + ep * p(t) + ew * w(t) + U(t) \qquad (21)$$

The stochastic error represented by $U(t)$ is added to make the model more realistic. The parameters a, *ep*, and *ew* are estimated by the least squares method so that (22) is minimized (consumption reduction is maximized).

$$\phi(a.ep.ew) = \sum_{i=1}^{T} U(t)^2 \sum_{i=1}^{T} [q(t) - (a + ep * p(t) + ew * w(t))]^2 \qquad (22)$$

To do so, simultaneous equations are obtained by setting the derivatives of the mentioned parameters equal to zero. The parameter values can be determined using simultaneous equations and past information of the study system.

D. Modeling the load response uncertainty using the IGDT method

In the IGDT method, the set of possible uncertainties is received; therefore, the objective function, which depends on uncertain parameters, is tried to be flexible against the input uncertainties.

In this section, the participation rate in the DRP is considered a non-deterministic parameter, and the controlling method of its effect on the problem is evaluated. So, according to the model, parameters γ_1 to γ_3 are non-deterministic.

The problem model is expressed in (23)-(26), considering the risk-aversion strategy. The risk-averse strategy is chosen because the problem is not risk-capable. The problem should be as resistant as possible to uncertainty of load participation, as the imbalance between generation and consumption will result from changes in the participation rate compared to that predicted in the risk-taking strategy. This is not acceptable for the grid operator.

$$\Re_C = \max_{X,\alpha} \alpha \qquad (23)$$

$$f < f_b(X,\gamma) \times (1+\beta), \gamma \in \Gamma \qquad (24)$$

$$f_b(X,\gamma) = \max_{X} f, \gamma = \bar{\gamma} \qquad (25)$$

$$\gamma = \bar{\gamma} \times (1-\alpha) \qquad (26)$$

where X is the decision variable including the spot prices and the value of the proposed load shedding, α is the radius of uncertainty, and β is the percentage of deviation from the objective function in the risk-aversion strategy.

E. Correlation handling between uncertain input variables

Uncertain variables may or may not be interdependent. When variables are interdependent, changes in one variable also affect other variables. The magnitude and direction of these effects are functions of this dependence. Generally, this issue is expressed through a covariance or correlation coefficient matrix. The correlation coefficients can be expressed in the form of (27):

$$\rho_{x,y} = \frac{\mathrm{cov}(x,y)}{\sigma_x \sigma_y} = \frac{E[(x-\mu_x)(y-\mu_y)]}{\sigma_x \sigma_y}$$
$$x, y = 1, 2, ..., n \qquad (27)$$

The correlation coefficient is positive +1 for perfect linear relationships and negative -1 for perfect linear relationships. In other relationships, the values between the [-1,1] range indicate the degree of linear dependence between variables. The variables have little dependence if the correlation coefficient is closer to zero. If the coefficient is close to 1 or -1, the correlation between the variables is stronger. The correlation is zero if the variables are independent, but the converse is invalid.

If the matrix *M* is a matrix of uncertain variables of the problem.

$$M = \begin{bmatrix} X_1 \\ X_2 \\ \vdots \\ X_N \end{bmatrix} \qquad (28)$$

The covariance matrix of the *M* vector obtained is equal to (29):

$$C_M = E(MM^T) = R \qquad (29)$$

In (29), R is a symmetric matrix, and it can be written according to the Cholesky decomposition method to obtain the value of L, where L is the Cholesky factor of a lower triangular matrix. To construct the correlation vector M, assume that W is a vector with N dimensions of an uncertain variable whose values are independent and whose variance is equal to one. Therefore, its covariance matrix is according to (30).

$$C_W = E(WW^T) = I \qquad (30)$$

Using the (30), the covariance matrix M can be written in the form of (31), and the correlation matrix M can be obtained.

$$C_M = E(\mathrm{MM}^T) = E(LWW^T L^T) = R \qquad (31)$$

Therefore, the correlation between the values of the uncertain vector M is applied.

F. Load management through CVR

One innovative method for reducing energy consumption and peak demand, without interfering with consumers' usage patterns, is CVR. This technique reduces the load by controlling the voltage at consumption buses to a minimum permissible value without compromising system security, as a significant portion of the electrical load is directly dependent on voltage.

Different types of loads respond to voltage drops in different ways. For instance, the power draw of cooling loads decreases when the voltage is reduced. However, these loads must operate for longer durations to reach the desired temperature because they are functioning at a lower power level. Consequently, their net energy consumption does not decrease. In contrast, the energy and power consumption of another category of loads often decreases with lower voltage. Meanwhile, constant-power loads experience almost no change in consumption due to a voltage change. Therefore, the responsiveness of a given grid to CVR depends on the models and characteristics of its constituent loads. Studies indicate that this method can reduce energy consumption by between 0.5% and 4%.

To investigate the impact of CVR on the problem of microgrid optimization, load flow equations must be considered alongside objective functions and constraints. The problem modeling includes a radial grid structure, voltage-dependent loads, an On-Load Tap Changer (OLTC) transformer, and shunt capacitors.

Recent studies have further demonstrated the effectiveness of CVR in modern distribution networks. For instance, [41] quantified the energy savings potential of CVR across different load compositions, while [42] proposed a real-time CVR algorithm considering voltage-dependent loads. More recently, [43] integrated CVR with deep reinforcement learning for volt-VAR optimization in unbalanced systems.

In a radial structure, the number of branches equals the number of nodes minus one. The system's primary bus, designated as bus 0, serves as the connection point between the distribution grid and the transmission system, maintaining a constant voltage range. Thus, the load flow equations for a branch are as follows.

$$P_{ij} - \sum_{k\in N_j} P_{jk} = \frac{r_{ij}\left(P_{ij}^2 + Q_{ij}^2\right)}{V_i^2} - p_j \tag{32}$$

$$Q_{ij} - \sum_{k\in N_j} Q_{jk} = \frac{x_{ij}\left(P_{ij}^2 + Q_{ij}^2\right)}{V_i^2} - q_j \tag{33}$$

$$V_i^2 - V_j^2 = 2\left(r_{ij}P_{ij} + x_{ij}Q_{ij}\right) - \frac{(r_{ij}^2 + x_{ij}^2)(P_{ij}^2 + Q_{ij}^2)}{V_i^2} \tag{34}$$

$$p_j = p_j^g - p_j^d\ , q_j = q_j^g - q_j^d + q_j^c \tag{35}$$

where i represents the bus number and p_j,q_j and v_j are the injected active power, injected reactive power, and voltage of this bus, respectively. Each line is marked with the subscript ij, where r_{ij}, x_{ij}, P_{ij} and Q_{ij} are the resistance, reactance, active power, and reactive power of line ij, respectively. The superscript d represents the load. The load is modeled using the ZIP model. So, the relationship between load value and voltage is as follows.

$$p_j^d(V_j) = P_{0,j}^d\left[P_{Z,j}\left(\frac{V_j}{V_{0,j}}\right)^2 + P_{I,j}\left(\frac{V_j}{V_{0,j}}\right) + P_{P,j}\right] \tag{36}$$

$$q_j^d(V_j) = Q_{0,j}^d\left[Q_{Z,j}\left(\frac{V_j}{V_{0,j}}\right)^2 + Q_{I,j}\left(\frac{V_j}{V_{0,j}}\right) + Q_{P,j}\right] \tag{37}$$

where the subscript 0 indicates the load value at nominal voltage, and the subscripts Z, I, and P indicate constant impedance, constant current, and constant power, respectively.

The model of transformers with OLTC is modeled as a device between buses ij. Its load distribution equations are as follows.

$$P_{ij} - \sum_{k\in N_j} P_{jk} = \frac{r_{ij}\left(P_{ij}^2 + Q_{ij}^2\right)}{V_i^2/a_{ij}^2} - p_j \tag{38}$$

$$Q_{ij} - \sum_{k\in N_j} Q_{jk} = \frac{r_{ij}\left(P_{ij}^2 + Q_{ij}^2\right)}{V_i^2/a_{ij}^2} - q_j \tag{39}$$

$$\frac{V_i^2}{a_{ij}^2} - V_j^2 = 2\left(r_{ij}P_{ij} + x_{ij}Q_{ij}\right) - \frac{\left(r_{ij}^2 + x_{ij}^2\right)\left(P_{ij}^2 + Q_{ij}^2\right)}{V_i^2/a_{ij}^2} \tag{40}$$

$$\underline{a}_{ij} \le a_{ij} \le \overline{a}_{ij} \tag{41}$$

where a_{ij} is the tap ratio of the transformer, whose value is limited to a minimum and maximum range.

Moreover, the shunt capacitor is modeled as a parallel susceptance in the corresponding bus, and the value of its injected reactive power depends on the voltage. This susceptance value is bounded between 0 and the maximum value.

$$q_i^c(V_i) = B_i^c V_i^2 \tag{42}$$

$$0 \le B_i^c \le \overline{B_i^c} \tag{43}$$

According to IEEE Std. 1547-2018, in terms of reactive power capacity and the ability to regulate the voltage, DG resources are divided into two groups: resources that have the least ability to control voltage within an acceptable value (this applies to systems with a low penetration coefficient) and those that have a more remarkable ability to regulate voltage (this applies to systems with a low penetration coefficient). In this study, the resources with high voltage control capacity are considered.

The active and reactive power outputs of these resources are constrained by their capability curves, which can be mathematically expressed by (44)-(46).

$$a1_i^r s_i^r \le p_i^g \le a2_i^r s_i^r \tag{44}$$

$$b1_i^r p_i^g \le q_i^g \le b2_i^r p_i^g \tag{45}$$

$$c1_i^r s_i^r \le q_i^g \le c2_i^r s_i^r \tag{46}$$

The voltage-power control of the source can be configured in four distinct operating modes: constant power factor, voltage-reactive power (V-Q), active power-reactive power (P-Q), and constant reactive power. The relationship between active and reactive power for each of these modes is modeled by (47)-(49), respectively.

$$q_i^g\left(p_i^g\right) = \tan(\emptyset_i) p_i^g \tag{47}$$

$$q_i^g(V_i) = -m_q\left(V_i - V_{i,ref}\right) \tag{48}$$

$$q_i^g\left(p_i^g\right) = -b_q\left(p_i^g - P_{rated}\right) \tag{49}$$

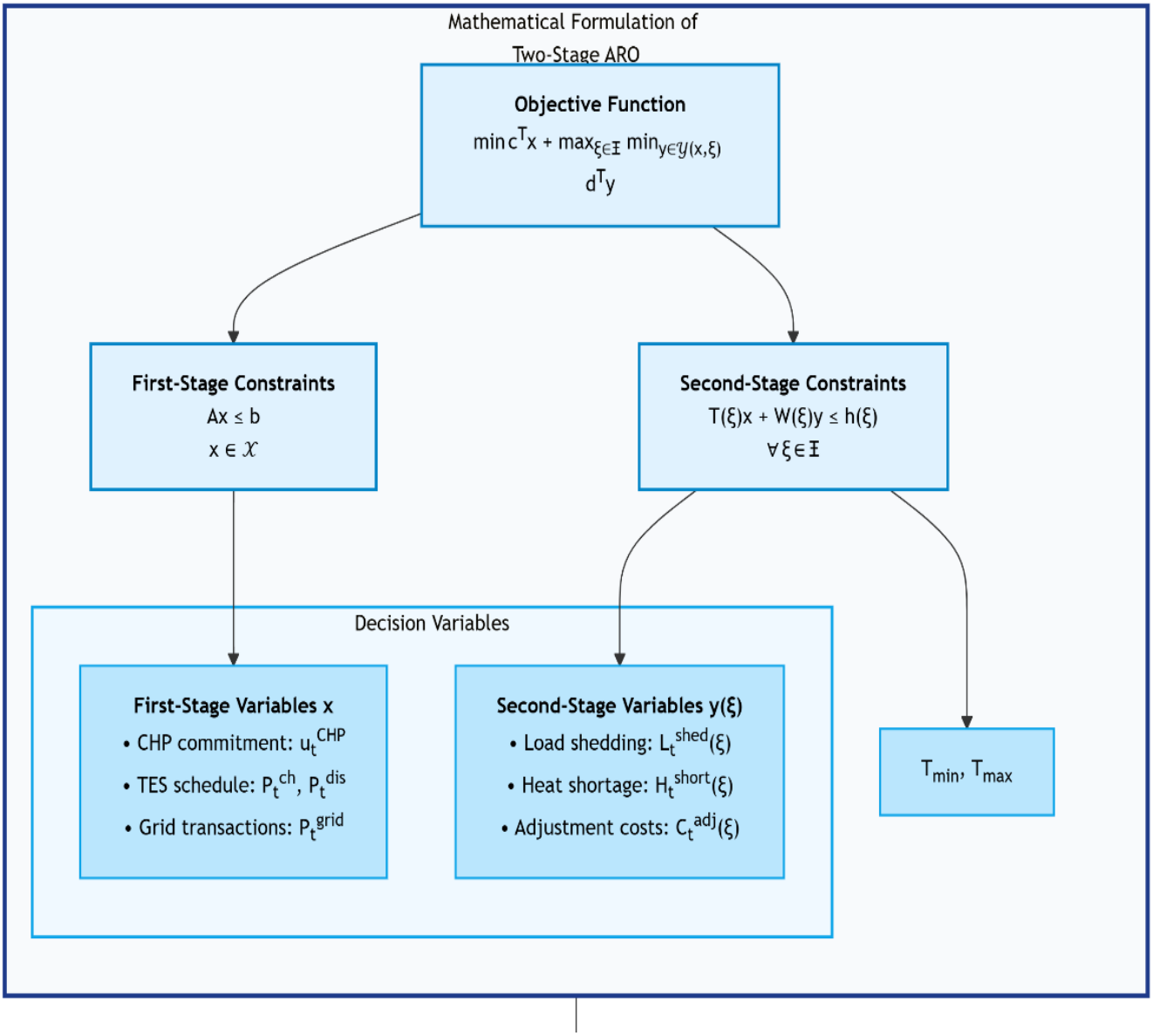

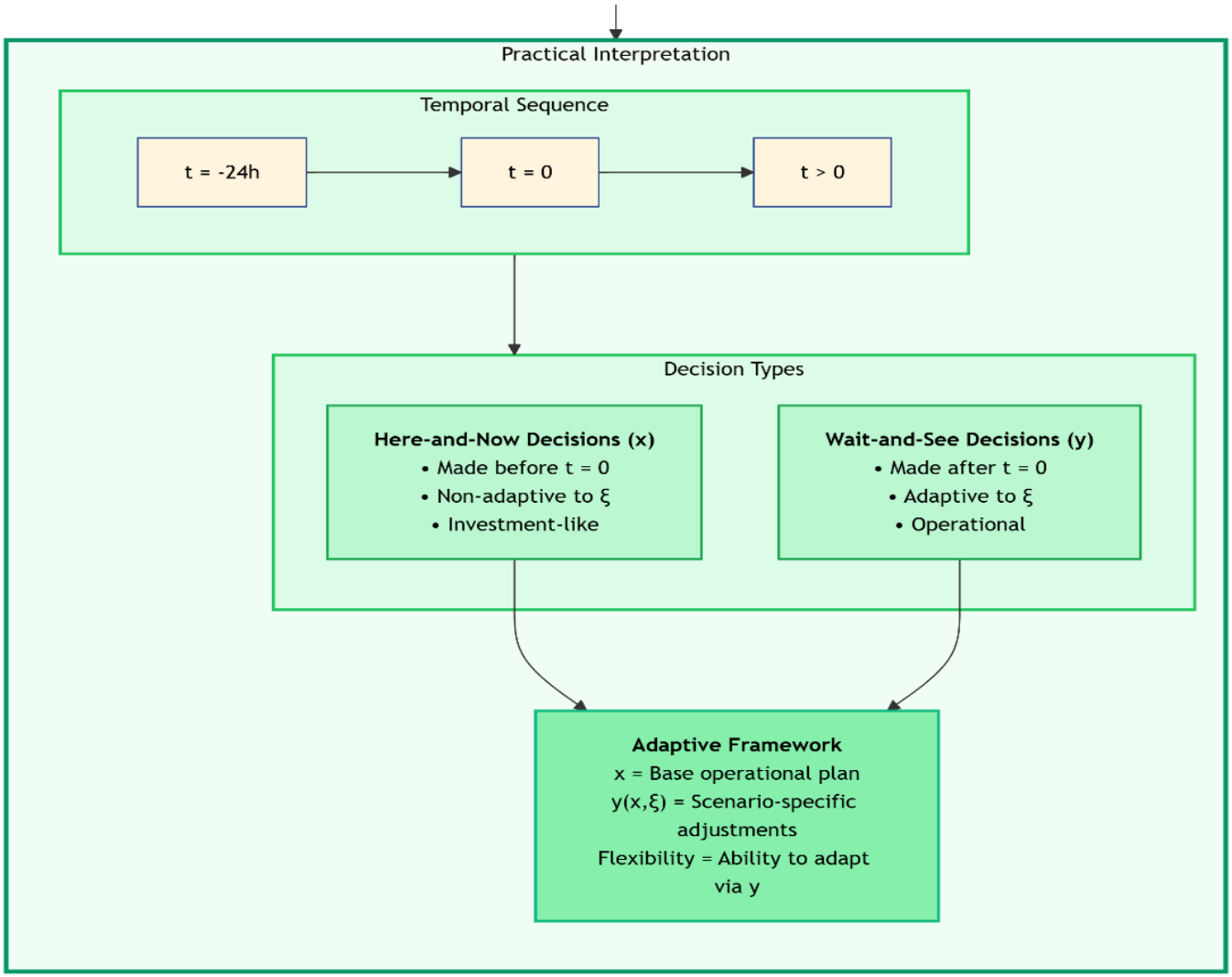

Fig. 1. Flowchart of the proposed two-stage fuzzy-IGDT optimization framework

The flowchart in Fig. 1 consists of two main stages: (1) IGDT-based uncertainty modeling for DR participation rates, including correlation handling via Cholesky decomposition; (2) Fuzzy multi-objective optimization with CVR, DR, and network constraints solved by a Genetic Algorithm. The feedback loop ensures convergence to a Pareto-optimal compromise solution.

III. . The Simulation Results

The scenarios for non-deterministic parameters—such as wind, load, solar irradiation, and generation resource data—are adopted from [8]. The grid topology will be detailed in the final section on numerical studies, where the results of the CVR analysis will be presented.

This study involves a numerical examination of a microgrid. The load profile and energy pricing characteristics of the upstream grid are provided in [2]. Figs. 2, 3, and 4 illustrate the TOU, RTP, and CPP programs, respectively. Subscribers within the microgrid consume power at a fixed tariff of 15 cents/kWh. The upstream grid rate refers to the price at which power is exchanged between the microgrid and the main grid.

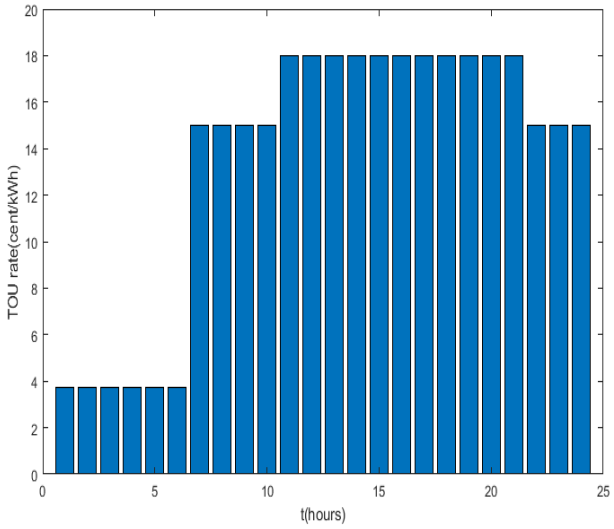

Fig. 2. TOU program

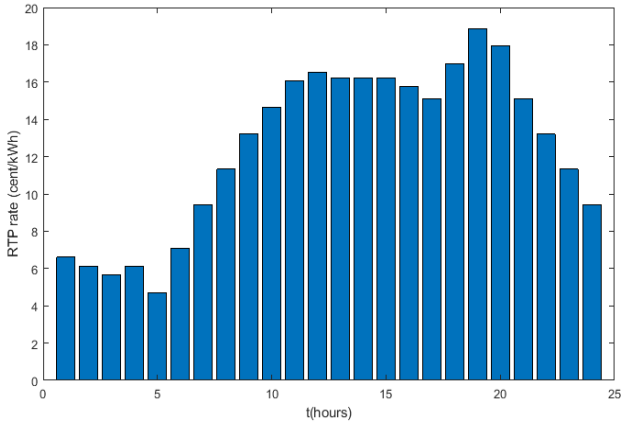

Fig. 3. RTP program

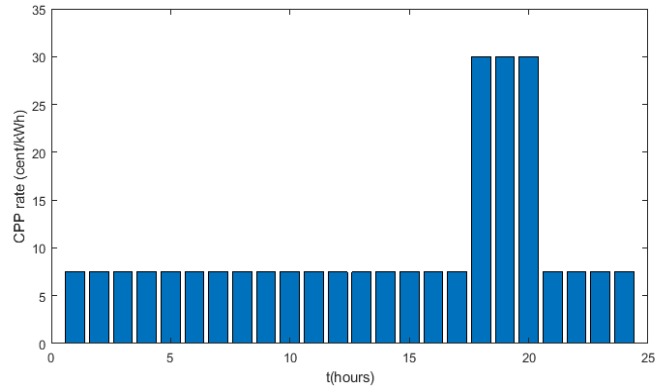

Fig. 4. CPP program

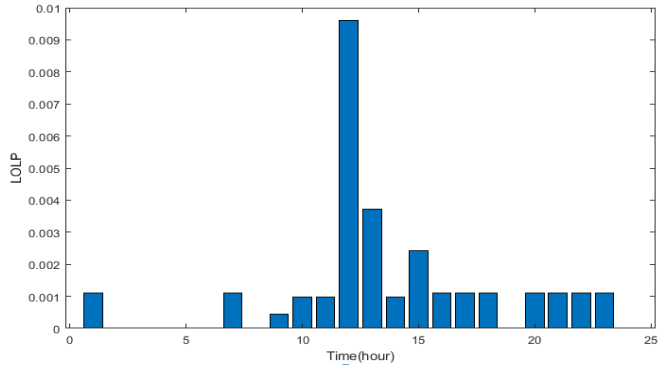

Fig. 5. Hourly LOLP with no load-shedding penalty

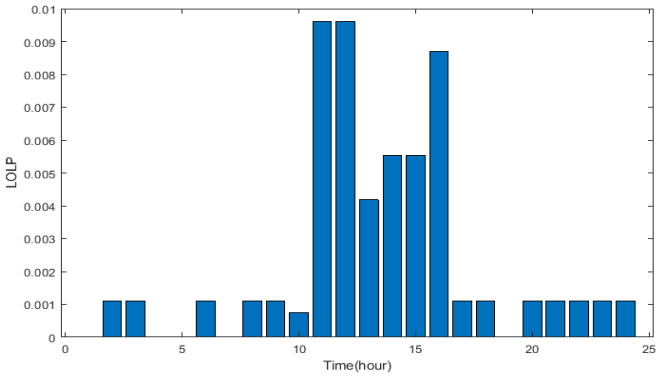

Fig. 6. Hourly LOLP with load-shedding penalty

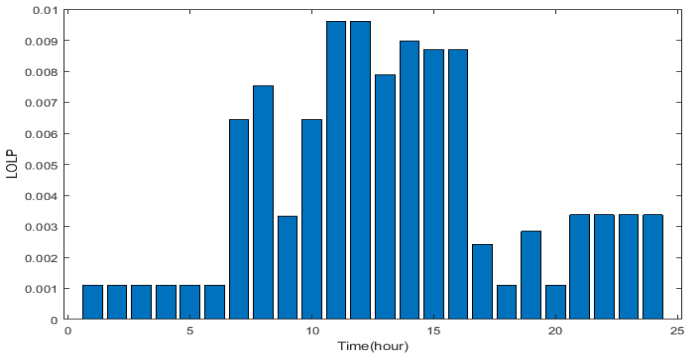

Fig. 7. Hourly LOLP with multi-target load-shedding penalty

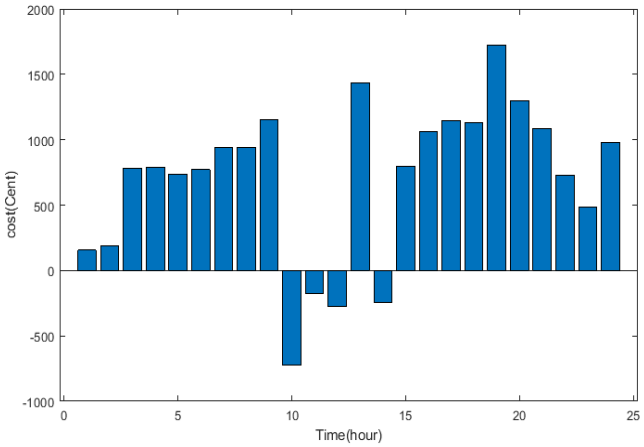

Fig. 8. Hourly cost with a multi-target load-shedding penalty

A. Simulation without considering DR

1. Numerical results with no load-shedding penalty

This section provides the hourly load supply cost, generation rate, and reservation value used in the GA. The total cost for this operational mode is 15,778.67 cents. The hourly LOLP is shown in Fig. 5. The expected energy loss over the 24 hours, as calculated by the GA, is 0.187 kWh.

2. Simulation results with load shedding penalty

The total cost of load supply in this mode is 16,703.97 cents, with the corresponding LOLP values illustrated in Fig. 6. The expected energy loss is calculated to be 0.357 kWh. It is important to note that the load interruption penalty and the reservation cost represent two directly conflicting objectives.

3. Simulation results with bi-objective load-shedding penalty

The total load supply cost in this mode is 16,902.19 cents, with the corresponding LOLP profile shown in Fig. 7. Fig. 8 shows the hourly cost with a multi-target load-shedding penalty. The expected energy loss is 0.263 kWh, resulting in a total cost of 16,902 cents. A comparative summary of the results from the three solution methods is presented in Table II. As illustrated in the table, the cost increases progressively across the case studies due to differing objective functions. In the first case study, where no load-shedding penalty is applied, the cost is minimized as the reservation is allocated solely to

meet the LOLP constraint. Consequently, the cost of this study is lower than that of the second study, which incorporates a load-shedding penalty into the objective function. This penalty leads to a higher cost but improves the reliability value, as seen in the second study's results.

Finally, the cost of the third study is higher than that of the single-objective second study. This is because the second study focuses exclusively on cost minimization, whereas the third study is a multi-objective optimization problem that balances cost and reliability objectives.

Here is a comparison of the total operational cost and EENS obtained from the proposed method with those reported in recent studies under similar microgrid conditions. Compared to [22], which used distributionally robust optimization without CVR, our method reduces cost by ≈11% (from 13,800 to 12,060 cents) while improving EENS by 18%. Relative to [23]'s deep reinforcement learning approach (cost ≈12,950 cents, EENS 0.29 kWh), our method achieves lower cost and better reliability due to explicit co-optimization of CVR and uncertainty-aware DR. These improvements stem from the synergistic effect of voltage-based load reduction and risk-averse DR participation modeling.

B. Simulation considering DR

The ambient temperature, which serves as the model for determining subscriber participation rates in the CPP program, is illustrated in Fig. 9. The parameters e_p and e_w, utilized in the CPP model, are set to -0.83 and 1.2085, respectively.

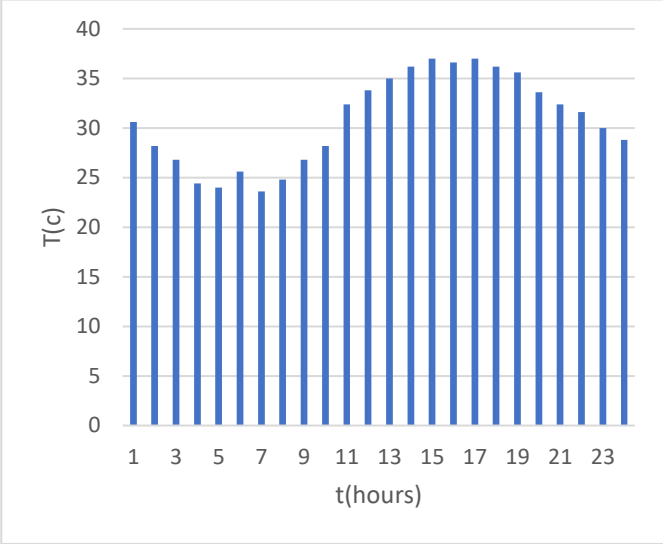

Fig. 9. The ambient temperature during 24 hours

TABLE II
The Comparison of Solutions

Algorithm	**Without penalty-single objective**		**With a penalty single objective**		**Bi-objective**	
	Cost	EENS	Cost	EENS	Cost	EENS
GA	15778	0.607	16702	0.478	16902	0.263

Figs. 10 and 11 depict the TOU programs under 5% and 10% participation scenarios, respectively. They show the application of these programs on the load curve and the resulting updated load available for shedding. For the pricing model, the critical peak parameters e_w and e_p are set to 1.2085 and -0.83, respectively. This analysis employs distinct 5% and 10% participation rates to better isolate and compare the effects of the TOU program.

TABLE III
The Comparison of the Cost of the Loads Participating in TOU Programs Before and After the Implementation of the Program (5%)

Program	**Cost before participation (cent)**	**Cost after participation (cent)**
TOU	1686.864	1520.229
RTP	1258.030	1022.785
CPP	1118.823	768.739

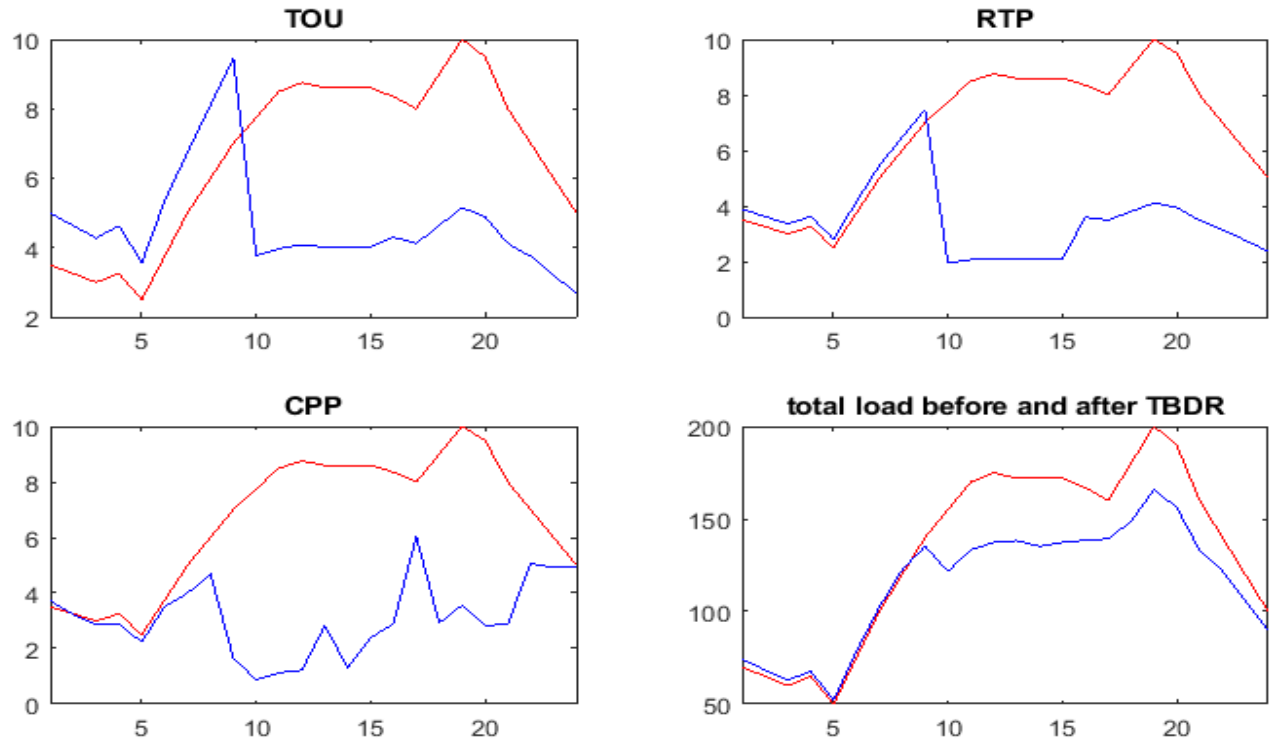

Figure 10. Updated load for 5% participation in the TOU programs

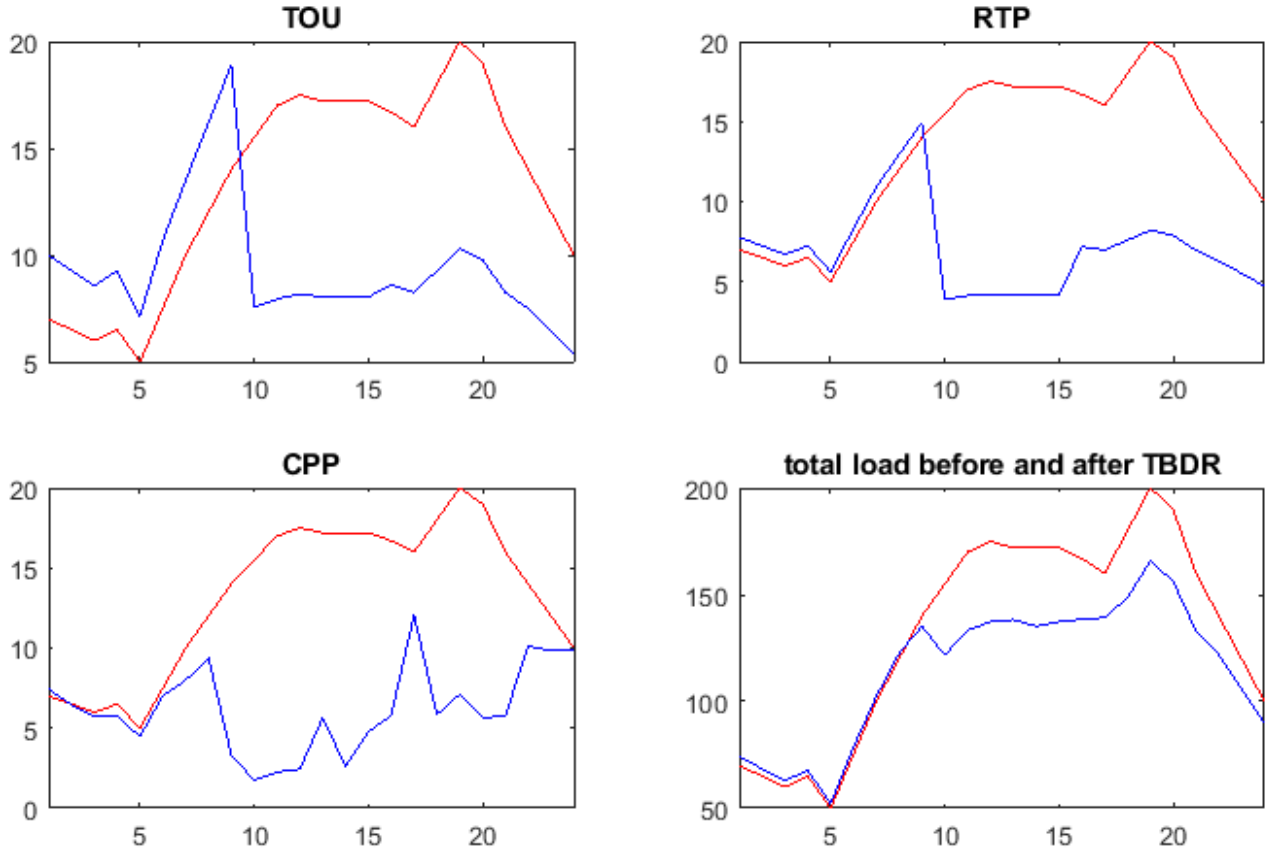

Figure 11. Updated load for 10% participation in the TOU programs

1. Simulation considering an interruptible load program and 5% participation in the TOU program

TABLE IV
The Comparison of the Cost of the Loads Participating in TOU Programs Before and After the Implementation of the Program (10%)

Program	Cost before participation (cent)	Cost after participation (cent)
TOU	3373.728	3040.457
RTP	2516.061	2045.571
CPP	2237.647	1537.479

TABLE V
Cost Objective Function Values for Different Demand Response Scenarios

Objective function	TOU program	Incentive-based program
16902	0	0
16423	5	10
12060	10	10

In the previous section, the cost of supplying electrical energy was a constant 45,793.5 cents. In this section, however, loads participate in demand-side programs voluntarily. Table III compares the costs for loads participating in TOU programs before and after implementation.

For such voluntary programs to be sustainable, their design must create a financial incentive for participants. This means the programs must generate more revenue (or greater savings) for the load than the total compensation paid to the generation resources. This economic viability ensures the programs can be repeatedly dispatched in the market. Under this voluntary participation model, the total cost is 16,423.78 cents.

2.Simulation considering an interruptible load program and 5% participation in the TOU program

A comparison of the costs for responsive demands, before and after program implementation, is provided in Table IV. For all three programs, the post-participation price is higher than the initial value, confirming the correct design of the DRP.

The value of the interruptible load, being a variable, is determined endogenously within the optimization process. This result will be presented subsequently. The total value of the cost function in this operational mode is 12,679.66 cents.

C. Adding the uncertainty of the contribution of responsive demands

This section employs info-gap decision theory to model the uncertainty associated with the participation of responsive demands in the programs. Previous analyses relied on fixed scenarios (0% and 10% for interruptible load; 5% and 10% for responsive demands) to demonstrate the impact of participation rates on the objective function. To deepen this analysis, three specific scenarios for responsive demands are modeled, as defined in Table V. The results of the objective function across these scenarios are also presented in Table V.

The data in Table V indicates that varying the participation rate has a minor effect on the objective function in the initial step, but a significant effect in the subsequent step. This non-linear and pronounced sensitivity underscores the necessity of explicitly accounting for this uncertainty. Since uncertainty in participation rates typically degrades the objective function's value, a risk-aversion strategy is implemented within the info-gap decision-making framework.

The goal of this strategy is to ensure the objective function remains robust against a predetermined degree of deviation in responsive demand participation from its forecasted value. The model is solved using this risk-averse approach, assuming a 10% deviation of responsive demands from their planned 10% participation level. The outcome, detailed in Table V, reveals that this 10% input deviation propagates to an approximately 40% degradation in the objective function from its base value of 12,060. This substantial performance amplification necessitates a method to mitigate such deviation.

To this end, a sensitivity analysis is conducted on the core info-gap parameters: the uncertainty radius of demand participation (α), the permissible relative deviation of the objective function (β), and the LOLP constraint. The total uncertainty radius (α) is allocated equally between incentive-based and time-based loads.

The first sensitivity analysis varies the allowable objective function deviation (β) from 5% to 15% in 2.5% increments, and the LOLP constraint from 1% to 5% in 1% increments. For each (β, LOLP) pair, the maximum feasible uncertainty radius (α) that satisfies these constraints is calculated; the results are presented in Fig. 10. Fig. 10 illustrates two key trade-offs:

1. For a given allowable cost deviation (β), a stricter reliability requirement (lower LOLP) necessitates a smaller tolerable uncertainty radius (α). Higher reliability demands greater predictability in demand participation.

2. For a given LOLP value, allowing for a larger performance sacrifice (higher β) permits a larger uncertainty radius (α). System robustness to uncertainty can be increased by accepting a higher potential cost.

Building on this, the changes in the maximum uncertainty radius (α) resulting from the variations in β and LOLP are further analyzed, yielding Fig. 12. Finally, by replotting the data from Fig. 12 with the objective function's percentage deviation on the horizontal axis, Fig. 12 is obtained to provide an alternative perspective on this relationship.

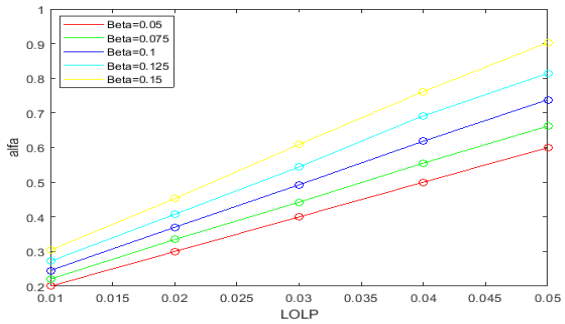

Fig. 12. Changes in the uncertainty radius in terms of LOLP changes for different βs

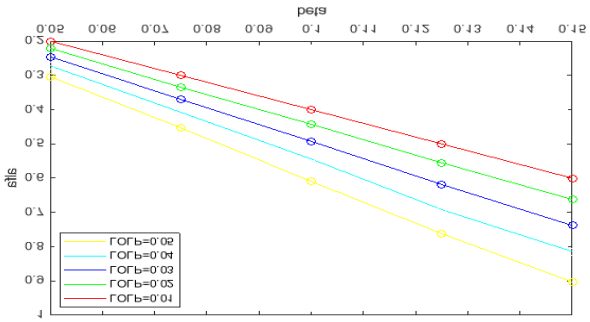

Fig. 13. Changes in the uncertainty radius in terms of β changes for different LOLPs

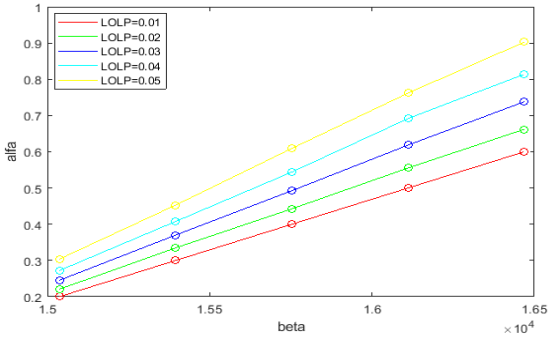

Fig. 14. Changes in the uncertainty radius in terms of generation cost changes for different LOLPs

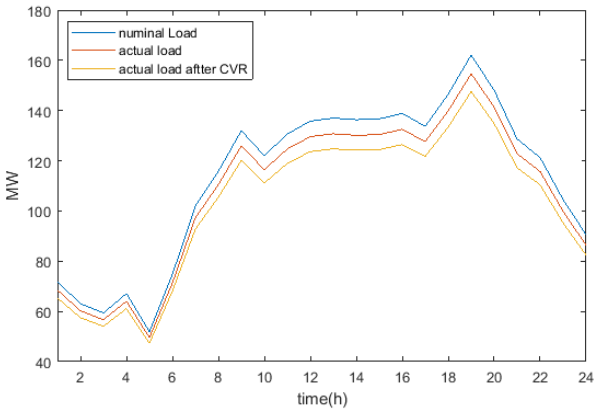

Fig. 15. The comparison of hourly load before and after applying CVR (after applying DR)

Fig. 13 confirms that the achievable uncertainty radius (α) contracts as the permissible LOLP limit becomes more stringent (decreases). Furthermore, the sensitivity of the acceptable uncertainty radius to the allowable cost increase (β) is negligible when β is small.

The analysis also reveals that for a given uncertainty radius, a higher desired reliability (lower LOLP) imposes greater operating costs on the system. This highlights the fundamental trade-off: simultaneously guaranteeing high reliability (low LOLP) and high robustness to uncertainty (large α) requires accepting a higher operating cost.

To quantify the advantage of the proposed risk-aversion strategy, two operational modes are compared:

- Mode 1 (Realization of Uncertainty): This mode assesses the cost if the actual demand participation deviates from the forecast. While the baseline cost was predicted to be 12,060 units, we now assume the participation scenario used in the risk-aversion strategy—a 5% deviation for each responsive demand—occurs. After accounting for corrections using the available spinning reserve, the total system cost rises to 13,982 units. This represents a cost increase of 1,922 units compared to the baseline.

- Mode 2 (Realization of Forecast): This mode assesses the opportunity cost if the forecast is perfectly accurate. Contrary to Mode 1, it is assumed that the predicted 10% participation is realized, but the system is dispatched using the more conservative risk-aversion strategy (which has a cost of 13,021 units). In this optimistic scenario, the actual cost of supplying the load would be 12,611 units. This means the system operator would have overpaid by 410 units compared to a perfect forecast.

The key finding is that the potential cost reduction in Mode 2 (410 units) is substantially smaller than the potential cost increase in Mode 1 (1,922 units). This asymmetry demonstrates that the risk-aversion strategy effectively shields the grid operator from severe financial downside. The operator accepts a small, known opportunity cost (overpayment if the forecast is perfect) to ensure against a much larger, uncertain cost penalty (underpayment if the forecast is wrong).

This is further evidenced by the result from Mode 1: the cost of 13,982 units, incurred when the forecast fails, is significantly higher than the 13,021 units calculated by the risk-aversion strategy. This confirms that if load participation uncertainty is not incorporated into DRPs, the system operator is likely to incur substantially higher costs in real-time operation than if a risk-averse strategy were employed.

D. Adding the grid effects and CVR

This section presents the test system used for the case study, including its topology and the technical specifications of its lines. The analysis is conducted on the standard IEEE 13-bus

test feeder. The hourly load profile remains consistent with that used in previous sections. For this study, the grid's active and reactive power demands are modeled using a ZIP load model to accurately represent their voltage dependence. Consequently, the final load consumption is expected to be slightly lower than the initial nominal load due to the effect of voltage reduction.

Following the implementation of CVR, the modified hourly grid load is calculated. Fig. 14 provides a comparative plot of the load profile under three conditions: the base case (before CVR), after applying CVR, and after implementing DR.

IV. Discussions

The key findings of this study are summarized as follows:

1. Impact of Load-Shedding Penalty on Cost: Incorporating a load-shedding penalty into the objective function increases the total cost of supplying load and spinning reserve. This is a direct result of adding a new cost component. To partially offset this increase, the optimization algorithm reduces the reserve capacity, which in turn increases the load-shedding index. This indicates that to genuinely improve reliability, the penalty for lost load must be set sufficiently high to deter the algorithm from compromising on reserve adequacy.

2. Interpretation of LOLP and Blackout Events: The low calculated value of the LOLP, relative to its permissible limit, suggests that blackouts are primarily caused by high-impact, low-probability events. While these events are rare, they result in the outage of significant load blocks, thereby substantially affecting the expected energy not supplied without drastically altering the probability index (LOLP) itself.

3. Scenario-Based Generation Planning: Generation planning was based on the most probable scenario, with incremental reserves allocated to cover shortages across various load, wind, and solar scenarios. It is noted that in certain scenarios, excess generation may occur, which could be curtailed from wind or solar sources.

4. Temporal Accuracy of Non-Deterministic Parameters: The proposed algorithm's short solution time (a few minutes) allows it to leverage the inherent increase in forecast accuracy as the operating horizon approaches. This enables highly precise predictions of non-deterministic parameters close to the dispatch time.

5. Cost-Reliability Trade-off via Expected Energy Loss: The balance between cost and reliability is best evaluated through the expected energy loss index. This metric, which is inherently cost-based, is integrated into the objective function alongside the cost of providing reserves, providing a unified framework for assessing the economic value of reliability.

6. Efficacy of DRPs: A significant improvement in both load supply cost and reliability indicators was achieved by incorporating responsive demands through DRPs. A key advantage is that the added cost associated with *announced* load shedding is negligible compared to the combined savings from reduced production/reserve costs and the avoidance of penalties for unannounced outages.

7. Value of the Risk-Aversion Strategy (IGDT): When modeling the uncertainty of demand participation using the IGDT method, employing a risk-aversion strategy exposes the system operator to a lower potential cost increase than the baseline mode. This demonstrates the strategy's effectiveness in managing uncertainty.

8. Cost of Ignoring Uncertainty: Conversely, if the uncertainty of load participation is not explicitly considered in the DRP design, the system operator is likely to incur higher actual operating costs than those projected by the risk-aversion strategy, especially as uncertainty increases.

9. Limited Impact of CVR on Cooling Loads: Incorporating grid effects and CVR revealed that the cooling load model had a negligible impact on net energy consumption. During peak hours (hot periods), a fixed amount of cooling energy is required. While CVR reduces instantaneous power, it also forces compressors to operate for longer durations to meet the cooling setpoint, resulting in minimal net energy savings for these loads.

10. CVR's Indirect Benefit for Demand Response: Although CVR does not reduce the energy consumption of cooling loads, it successfully reduces their instantaneous power demand. This power reduction contributes to overall peak shaving and positively affects the demand response potential, with an observed impact of approximately 3%.

V. Conclusion

This paper proposed a comprehensive two-stage fuzzy-based multi-objective optimization framework for day-ahead scheduling of active distribution networks, integrating Conservation Voltage Reduction (CVR), uncertainty-aware Demand Response Programs (DRPs), Smart Transformers, and Soft Open Points (SOPs). The main achievements of the proposed method are:

- Simultaneous co-optimization of economic (operational cost) and technical (voltage stability, voltage deviation, feeder loading) objectives using a fuzzy goal programming approach.
- Explicit modeling of load participation uncertainty in DRPs via Information Gap Decision Theory (IGDT) with a risk-averse strategy, which was shown to avoid up to 1,922 units of cost increase compared to ignoring uncertainty.
- Demonstration that CVR provides peak reduction (≈3%) even for cooling loads, despite limited net energy savings, and that coordination with DR improves both reliability and cost.

- Introduction of two complementary reliability criteria: LOLP (probability-based) and EENS × VOLL (cost-based), where LOLP serves as a hard constraint, and EENS × VOLL is part of the objective, allowing explicit trade-off between reserve cost and outage penalty.

Future research directions are:

- ✓ Incorporating correlation between uncertain sources (wind, solar, load) in scenario generation.
- ✓ Designing dynamic, risk-based prices for DRPs based on IGDT uncertainty radius.
- ✓ Applying IGDT directly to wind, load, and stress uncertainties instead of scenario-based methods.
- ✓ Implementing CVR in larger, weak radial networks with voltage constraints.

FUNDING STATEMENT

This research received no specific grant from any funding agency in the public, commercial, or not-for-profit sectors.

CONFLICTS OF INTEREST

The author declares no conflict of interest regarding the publication of this article.

AUTHORS' CONTRIBUTIONS

All authors contributed equally to this work.

STATEMENT ON THE USE OF GENERATIVE AI

Deepseek (AI tool) was used only for language editing and grammar improvement of the paper, and the authors have reviewed AI outputs carefully.

REFERENCES

[1] MO. Ellabban, H. Abu-Rub, and F. Blaabjerg, "Renewable energy resources: Current status, future prospects and their enabling technology," *Renew. Sustain. Energy Rev.* 39 748-764 (2014).

[2] T. Lehtola and A. Zahedi, "Technical challenges in the application of renewable energy: A review," *Int. J. Smart Grid Clean Energy* 9(3) 689-699 (2020).

[3] M. Resch, A. Schuller, and C. M. Schäfer, "Techno-economic assessment of flexibility options versus grid expansion in distribution grids," *IEEE Trans. Power Syst.* 36(5) 3830-3839 (2021).

[4] B. N. Silva, M. Khan, and K. Han, "Futuristic sustainable energy management in smart environments: A review of peak load shaving and demand response strategies, challenges, and opportunities," *Sustainability* 12(14) 5561 (2020).

[5] J. O. Petinrin and M. Shaaban, "Impact of renewable generation on voltage control in distribution systems," *Renew. Sustain. Energy Rev.* 65 770-783 (2016).

[6] T. Broeer, J. Fuller, F. Tuffner, D. Chassin, and N. Djilali, "Modeling framework and validation of a smart grid and demand response system for wind power integration," *Appl. Energy* 113 199-207 (2014).

[7] A. G. Madureira and J. P. S. Catalão, "A Two-Stage Stochastic Model for Day-Ahead Scheduling of Microgrids with CVR and Demand Response under Uncertainty," *IEEE Trans. Power Syst* 36(5) 4120-4133 (2021).

[8] J. S. Vardakas, N. Zorba, and C. V. Verikoukis, "A Survey on Demand Response Programs in Smart Grids: Pricing Methods and Optimization Algorithms," *IEEE Commun. Surv. Tutor.* 17(1) 152-178 (2015).

[9] S. Das and M. Basu, "Day-ahead optimal bidding strategy of microgrid with demand response program considering uncertainties and outages of renewable energy resources," *Energy* 190 116441 (2020).

[10] P. Singh, A. K. Bohre, and A. K. Singh, "Moth search optimization for optimal DERs integration in conjunction to OLTC tap operations in distribution systems," *IEEE Syst. J.* 14(1) 880-888 (2019).

[11] J. Wang, "Analysis of energy savings of CVR including thermostatic loads in distribution systems," in *Proc. 2018 IEEE Power Energy Soc. Gen. Meet. (PESGM)* (2018).

[12] A. Fakour et al., "Investigating Impacts of CVR and Demand Response Operations on a Bi-Level Market-Clearing With a Dynamic Nodal Pricing," *IEEE Access* 11 19148-19161 (2023).

[13] K. Gholami, A. Azizivahed, A. Arefi, and L. Li, "Risk-averse Volt-VAr management scheme to coordinate distributed energy resources with demand response program," *Int. J. Elect. Power Energy Syst.* 146 108713 (2023).

[14] M. S. H. Nizami, M. J. Hossain, and K. Mahmud, "A Coordinated Electric Vehicle Management System for Grid-Support Services in Residential Networks," *IEEE Syst. J.* 15(2) 2066-2077 (2021).

[15] İ. Şengor, O. Erdinç, B. Yener, and A. Taşcıkaraoglu, "Optimal Energy Management of EV Parking Lots Under Peak Load Reduction Based DR Programs Considering Uncertainty," *IEEE Trans. Sustain. Energy* 10(3) 1034-1043 (2019).

[16] X. Wang et al., "A two-layer control strategy for soft open points considering the economical operation area of transformers in active distribution networks," *IEEE Trans. Sustain. Energy* 1-12 (2022).

[17] A. Singh and A. Maulik, "Energy management of distribution network in the presence of smart transformers, soft open points, and battery energy storage system," in *Proc. 2022 Int. Conf. Power Energy Syst. Appl. (ICoPESA)* 437-442 (2022).

[18] K. Thirugnanam, M. S. E. Moursi, V. Khadkikar, and H. H. Zeineldin, "Energy Management of Grid Interconnected Multi-Microgrids Based on P2P Energy Exchange: A Data Driven Approach," *IEEE Trans. Power Syst.* 36(2) 1546-1562 (2021).

[19] A. U. Rehman et al., "An Optimal Power Usage Scheduling in Smart Grid Integrated with Renewable Energy Sources for Energy Management," *IEEE Access* 9 84619-84638 (2021).

[20] S. Ali et al., "Energy Management in High RER Multi-Microgrid System via Energy Trading and Storage Optimization," *IEEE Access* 10 6541-6554 (2022).

[21] G. Mohy-ud-din, K. M. Muttaqi, and D. Sutanto, "Adaptive and Predictive Energy Management Strategy for Real-Time Optimal Power Dispatch From VPPs Integrated With Renewable Energy and Energy Storage," *IEEE Trans. Ind. Appl.* 57(3) 1958-1972 (2021).

[22] J. Smith, L. Brown, and K. Johnson, "A Distributionally Robust Optimization Framework for Demand Response under Renewable Uncertainty," *IEEE Trans. Smart Grid* 15(1) 450-462 (2024).

[23] H. Chen and Y. Wang, "Deep Reinforcement Learning for Real-Time Demand Response in PV-Rich Microgrids," *Appl. Energy* 355 122235 (2024).

[24] M. Kermani, E. Shirdare, G. Parise, M. Bongiorno, and L. Martirano, "A Comprehensive Technoeconomic Solution for Demand Control in Ports: Energy Storage Systems Integration," *IEEE Trans. Ind. Appl.* 58(2) 1592-1601 (2022).

[25] D. Yan, H. Yin, T. Li, and C. Ma, "A Two-Stage Scheme for Both Power Allocation and EV Charging Coordination in a Grid-Tied PV–Battery Charging Station," *IEEE Trans. Ind. Informat.* 17(10) 6994-7004 (2021).

[26] L. Mohammadian, "Integrating Renewable Energy and Demand Response Strategies for Cost-Effective Industrial Energy Management", *Journal of Artificial Intelligence in Electrical Engineering*. 13(52):16-25 (2025).

[27] M. Pertl, F. Carducci, M. Tabone, M. Marinelli, S. Kiliccote, and E. C. Kara, "An Equivalent Time-Variant Storage Model to Harness EV Flexibility: Forecast and Aggregation," *IEEE Trans. Ind. Informat.* 15(4) 1899-1910 (2019).

[28] S. Rafique, M. J. Hossain, M. S. H. Nizami, U. B. Irshad, and S. C. Mukhopadhyay, "Energy Management Systems for Residential Buildings with Electric Vehicles and Distributed Energy Resources," *IEEE Access* 9 46997-47007 (2021).

[29] S. Zhou, Z. Chen, D. Huang, and T. Lin, "Model Prediction and Rule Based Energy Management Strategy for a Plug-in Hybrid Electric Vehicle With Hybrid Energy Storage System," *IEEE Trans. Power Electron.* 36(5) 5926-5940 (2021).

[30] R. Jones, P. Davis, and T. Wilson, "A Bi-Level Market Framework for V2G Service Aggregation from Autonomous EV Fleets," *IEEE Trans. Transport. Electrific.* 10(2) 2100-2115 (2024).

[31] F. O. Ramos, A. L. Pinheiro, R. N. Lima, M. M. B. Neto, W. A. S. Junior, and L. G. S. Bezerra, "A Real Case Analysis of a Battery Energy Storage System for Energy Time Shift, Demand Management, and Reactive Control," in 2021 IEEE PES Innov. Smart Grid Technol. Conf. - Latin America (ISGT Latin America) 1-5 (2021).

[32] H. Farham, L. Mohammadian, H. Alipour, J. Pouladi, "Energy procurement of large industrial consumer via interval optimization approach considering peak demand management", *Sustainable Cities and Society*, Vol. 46, 101421, (2019), https://doi.org/10.1016/j.scs.2019.101421.

[33] H. Chen, R. Xiong, C. Lin, and W. Shen, "Model predictive control based real-time energy management for hybrid energy storage system," *CSEE J. Power Energy Syst.* 7(4) 862-874 (2021).

[34] E. Mokaramian, H. Shayeghi, F. Sedaghati, A. Safari, and H. H. Alhelou, "An Optimal Energy Hub Management Integrated EVs and RES Based on Three-Stage Model Considering Various Uncertainties," *IEEE Access* 10 17349-17365 (2022).

[35] R. R. Avula, J.-X. Chin, T. J. Oechtering, G. Hug, and D. Mansson, "Design Framework for Privacy-Aware Demand-Side Management with Realistic Energy Storage Model," *IEEE Trans. Smart Grid* 12(4) 3503-3513 (2021).

[36] Q. Li and W. Zhang, "Federated Learning-Based Model Predictive Control for Privacy-Preserving Multi-Microgrid Operations," *IEEE Trans. Power Syst.* 40(1) 550-561 (2025).

[37] Z. Zhang, Y. Huang, Z. Chen, and W.-J. Lee, "Integrated Demand Response for Microgrids With Incentive Compatible Bidding Mechanism," *IEEE Trans. Ind. Appl.* 59(1) 118-127 (2023).

[38] L. Mohammadian , T. Abedinzadeh and H. Helmi, "A Bi-Level Optimization Framework for Multi-Objective Energy Management in Active Distribution Networks," *Journal of Modeling in Engineering*, (2026): -, doi: 10.22075/jme.2026.39378.2919

[39] Z. Yang, H. Tian, H. Min, F. Yang, W. Hu, L. Su, and S. SaeidNahaei, "Optimal microgrid programming based on an energy storage system, price-based demand response, and distributed renewable energy resources," *Util. Policy* 80 101474 (2023).

[40] S. Kumar, A. Patel, and M. Thompson, "Multi-Agent Deep Reinforcement Learning for Joint CVR and Soft Open Point Optimization in Unbalanced Distribution Networks," *IEEE Trans. Smart Grid* 16(1) 720-732 (2025).

[41] A. Pardasani, B. Djokic, Y. Hu, P. Stymiest, S. Goss, and K. Goggin, "Evaluation of Conservation Voltage Reduction (CVR) in New Brunswick, Canada," 2024 IEEE Power & Energy Society General Meeting (PESGM), Seattle, WA, USA, pp. 1-5, (2024), doi: 10.1109/PESGM51994.2024.10688709.

[42] Sh.Pourfarzin, T. Daemi, H. Akbari, "Technoeconomic Conservation Voltage Reduction–Based Demand Response Approach to Control Distributed Power Networks", *International Transactions on Electrical Energy Systems*, 2024, 9752955, 21 pages, (2024). https://doi.org/10.1155/2024/9752955

[43] A. Gorjian, M. Eskandari, and M.H. Moradi, "Multi-agent deep reinforcement learning for joint dynamic conservation voltage reduction and Q-sharing in inverter-based autonomous microgrids," *Electric Power Systems Research*, vol. 231, 110333, (2024). Doi:10.1016/j.epsr.2024.110333